CO$_2$ reforming of methane as a source of hydrogen using a membrane reactor

J. Múnera, S. Irusta, L. Cornaglia, E. Lombardo[*]

Instituto de Investigaciones en Catálisis y Petroquímica (FIQ, UNL-CONICET) INCAPE, Santiago del Estero 2829, 3000 Santa Fe, Argentina

Abstract

The catalytic production of hydrogen through the carbon dioxide reforming of methane was carried out both in a plug-flow reactor and in a dense Pd/Ag membrane reactor. In the former device, the activity and stability of Pt/La$_2$O$_3$ were investigated and compared to the Rh/La$_2$O$_3$ solids. None of the catalysts assayed showed carbon deposition through TGA although the Raman spectra always included weak bands assigned to graphitic carbon. The best Pt and Rh catalysts were used in the membrane reactor and in both cases significant increases in CH$_4$ and CO$_2$ conversions were recorded. Despite their similar activities, the Rh (0.2%)/La$_2$O$_3$ was much more stable than the Pt/La$_2$O$_3$ formulations. The origin of the deactivation was found to be the partial sintering of the platinum after 100 h on stream at 823 K. Rh interacted more strongly with the support and this impaired the sintering of the well-dispersed metal.
© 2002 Elsevier Science B.V. All rights reserved.

Keywords: CO$_2$ reforming; Pt and Rh; Membrane reactor

1. Introduction

Many of the membrane reactors studied have used non-porous Pd alloy membranes, which allow the completely selective permeation of H$_2$ [1]. The most widely studied application of these membranes is the equilibrium shifting in hydrocarbon dehydrogenation [2].

Hydrogen permselective membranes have been used in membrane reactors for steam reforming [3–5]. This reaction has also been simulated for a dense Pd/Ag composite membrane and a series of microporous membranes [6]. The influence of various process

parameters on the reactor performance, and a comparison of the process economics with state-of-the-art hydrogen plants were carried out by Petersen et al. [7].

A porous Vycor glass membrane [8] and a defect free zeolite membrane [9] were tested for CO$_2$ reforming. Prabhu et al. [10] developed a mathematical model to simulate the performance of a fixed-bed reactor, and of both a partially selective and a totally selective membrane reactor.

The carbon dioxide reforming of methane was studied by Kikuchi and Chen [11] using a commercial Ni catalyst and supported Ru, Pd, Ir and Pt catalysts in a hydrogen-permeable membrane reactor. In all cases, they found abundant coke deposition. These authors concluded that the membrane reactor effectively promotes CO$_2$ reforming. Galuszka et al. [12],

* Corresponding author. Tel.: +54-342-4536861;
fax: +54-342-4571162.
E-mail address: nfisico@fiqus.unl.edu.ar (E. Lombardo).

using a reactor with a dense palladium membrane, demonstrated the enhancement of the CH_4 conversion beyond the limits imposed by equilibrium thermodynamics. However, after 20 h of being exposed to CH_4, H_2, CO, CO_2 and H_2O at 823–923 K, the Pd membrane presented swelling and development of porosity. These authors also found that the corrosion of the top layer of Pd by filamentous carbon formation was quite pronounced. They concluded that metallic membranes are likely to have no application in this system due to carbon deposition and filamentous carbon formation that inevitably leads to membrane destruction. Appropriate catalysts preventing carbon deposits formation are needed to avoid this problem.

Rh/La_2O_3 catalysts were found to be stable and presented low carbon deposition at 823 K [13]. Pt is one of the most active and stable metals used in the CO_2 reforming of methane [14–17]. The stability of Pt in this reaction crucially depends on the support. The major cause of deactivation is the blocking of active sites by carbon deposited from methane [14]. CO_2 might be adsorbed and activated through the formation of carbonate on the surface of zirconia [17]. In the same way, La_2O_3 could enhance the activation of CO_2 adsorbed, thus facilitating the reforming reaction and hindering the deposition of carbon.

In this work, the activity and stability of Pt/La_2O_3 catalysts for the dry reforming of methane is studied in a plug-flow reactor. These catalysts and the Rh/La_2O_3

formulations were used in a Pd/Ag membrane reactor. Both the fresh and used catalysts were characterized by TPR, DRX and Raman spectroscopy. The metal dispersion was determined by H_2 chemisorption and TPD.

2. Experimental

2.1. Catalyst preparation

Catalysts were prepared by the conventional wet impregnation of La_2O_3 (Anedra 99.99%) using H_2 $(PtCl_6) \cdot 6H_2O$, Pt $(NH_3)_4(NO_3)_2$ and $RhCl_3 \cdot 3H_2O$ as precursor compounds. In all cases, the resulting suspension was then heated at 353 K to evaporate the water, and the solid material was dried in an oven at 383 K overnight. The resulting catalysts were calcined for 6 h at 823 K. The Rh (0.2%) and Pt (1%) catalysts supported on SiO_2 were prepared for the TPR experiments.

2.2. Catalyst testing

For fixed-bed reactor experiments the catalyst (50 mg) was loaded into a tubular quartz reactor (i.d. 5 mm), which was placed in an electric oven. The double tubular membrane reactor (Fig. 1) was built using a commercial dense Pd/Ag alloy (inner tube),
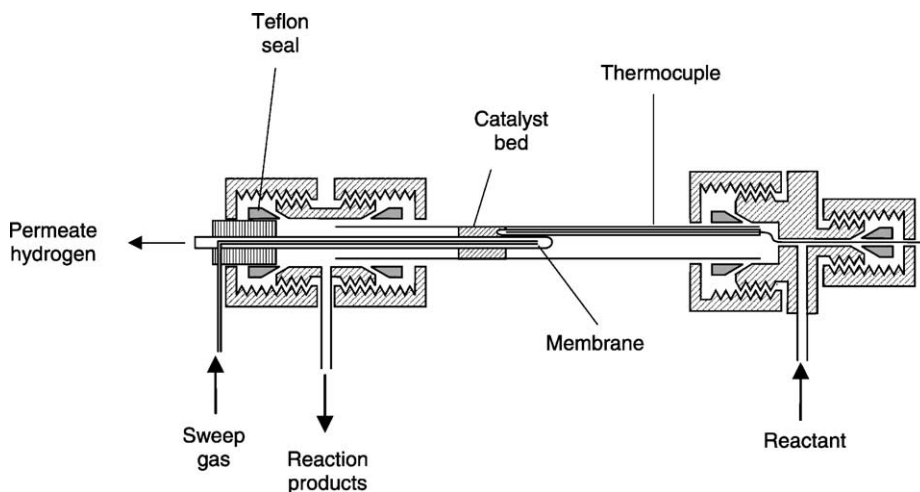

Fig. 1. Reactor scheme.

provided by REB Research and Consulting, with one end closed and an inner tube to allow helium sweep gas flow. The outer tube was made of commercial non-porous quartz (i.d. 9 mm). The catalyst, diluted with quartz chips to achieve a bed height of 3 cm, was packed in the outer annular region (shell side). The inner side of the membrane in all runs was kept at atmospheric pressure. The catalysts were heated in He at 823 K and then reduced in situ in H_2 at the same temperature for 2 h. After reduction, the feed stream gas mixture (33 vol.% CH_4, 33 vol.% CO_2, 34 vol.% He, $P = 1$ atm) was switched through the reactor.

To measure the equilibrium conversions, the membrane reactor was operated with no sweep gas and no pressure difference between the tube and the shell sides. In this case, the conversions were measured after a 12 h stabilization period.

The reaction products and the permeated mixture were analyzed with a TCD gas chromatograph equipped with a Porapak and a molecular sieve column and with an on-line Balzers Quadstar TU 422 mass spectrometer previously calibrated for each gas. The carbon balance was close to one in all cases.

2.3. Membrane characterization

The H_2 permeance through the Pd/Ag membrane was investigated at different trans-membrane pressures and sweep gas flow rates. The reactor filled with quartz wool was heated in He flow to 823 K and then the feed was switched to pure hydrogen or H_2/He mixtures. The permeate pressure in all runs was kept constant at 1 atm. Hydrogen was measured with an on-line Balzers Quadstar TU 422 mass spectrometer.

2.4. Metal dispersion and X-ray diffraction (XRD)

The Rh and Pt dispersion of the fresh catalysts, following the H_2 reduction at 973 K for 0.5 h, was determined by static equilibrium H_2 adsorption at room temperature in a conventional vacuum system.

H_2 desorption experiments were carried out using a flow reactor. This procedure was as follows: after reduction at 973 K for 0.5 h, the catalyst was rapidly cooled to 573 K in He, exposed to H_2 flow for 1 h, and then cooled to 300 K and maintained for 30 min under H_2 flow. The feed was switched to He and the desorb-ing H_2 was measured with an on-line mass spectrometer.

The XRD patterns of the calcined and used solids were obtained with an XD-D1 Shimadzu instrument, using Cu Kα radiation at 35 kV and 40 mA. The scan rate was $1°min^{-1}$ for values between $2\theta = 10$ and $80°$.

2.5. Temperature-programmed reduction (TPR)

An Ohkura TP-20022S instrument equipped with TCD was used for the TPR experiments. To eliminate the carbonates present in the samples, two different pretreatments were used: (i) the samples were heated up to 1123 K in oxygen flow, then this temperature was kept constant for 1 h; (ii) the samples were heated up to 823 K in oxygen flow, kept constant for 2 h and then, were cooled down in Ar flow. Afterwards, they were reduced in a 5% H_2–Ar stream, with a heating rate of 10 K min^{-1} up to the maximum treatment temperature.

2.6. Thermogravimetric analysis

The absence of carbon on the used catalysts was determined by oxidizing the carbon in a Mettler Toledo TGA/SDTA (Model 851) system. The used catalysts (usually 10 mg) were heated at 10 K min^{-1} to 1173 K in a flow of 90 ml min^{-1} air.

2.7. Laser Raman spectroscopy (LRS)

The Raman spectra were recorded with a TRS-600-SZ-P Jasco Laser Raman instrument, equipped with a charge coupled device (CCD) with the detector cooled to about 153 K using liquid N_2. The excitation source was the 514.5 nm line of a Spectra 9000 Photometrics Ar ion laser. The laser power was set at 30 Mw.

3. Results and discussion

3.1. Activity and stability measurements in fixed-bed reactor

The reaction rates obtained at 823 K for all the catalysts are reported in Table 1. Note that the increase of the Rh content from 0.2 to 0.6% only slightly improves the performance. However, in the case of Pt supported

Table 1
Catalytic behavior, dispersion and reducibility of La supported solids

Catalysts[a]	H/M[b]	R_{CH_4} (mol h^{-1} g^{-1})[c]	R_{CO_2} (mol h^{-1} g^{-1})[c]	TOF (s^{-1})			TPR		
				CH$_4$	CO$_2$	$T^{d,e}$ (K)	H$_2$/M[e]	$T^{d,f}$ (K)	H$_2$/M
Rh (0.2)	0.64	0.16	0.33	3.6	7.4	433, 490	0.82	481, 545	0.88
Rh (0.6)	0.14	0.18	0.45	6.1	15.3	420, 458	1.08	482, 546	0.49
Pt (0.41)[g]	0.29	0.07	0.19	1.4	3.8	407, 473(sh), 560	1.02	580	1.50
Pt (0.79)[g]	–	0.09	0.28	–	–	390, 550	0.75	590	0.87
Pt (0.94)[g]	0.19	0.12	0.25	3.6	7.5	412, 473, 603	0.65	595	1.50
Pt (0.93)[h]	0.17	0.12	0.27	4.1	9.2	410(sh), 528, 618	2.17	621	1.83
Pt (2.35)[h]	0.05	0.24	0.36	10.9	16.4	445, 480	1.80	618	1.85

[a] Weight percent are in brackets.

[b] Calculated by H$_2$ chemisorption.

[c] Reaction rates at 823 K, 33 vol.% CH$_4$, 33 vol.% CO$_2$, 34 vol.% He, $P = 1$ atm.

[d] Reduction temperature.

[e] Treatment temperature: 823 K.

[f] Treatment temperature: 1123 K.

[g] Pt (NH$_3$)$_4$ (NO$_3$)$_2$ as precursor.

[h] H$_2$(PtCl$_6$)6H$_2$O as precursor.

catalysts, the methane reaction rate increases linearly with the Pt loading.

The determination of metal dispersion in monometallic Rh and Pt catalysts was performed after reduction at 973 K followed by evacuation at 773 K for 1 h to complete H$_2$ desorption after reduction. The H/metal ratios obtained are shown in Table 1. There is good agreement between this ratio obtained through hydrogen TPD experiments and the one measured by hydrogen chemisorption. Reduction treatments at 823 K lead to similar dispersion values. With this dispersion, the TOF (Table 1) was estimated as proposed by Mork and Maier [18].

Conversion values were used to evaluate catalyst stability. The Rh supported catalysts showed practically no loss of activity, over a testing period of 100 h at 823 K [13]. However, the Pt (0.93%) catalyst exhibited a significant loss of activity after 24 h on stream (Fig. 2).

In all our catalysts, no carbon deposition was observed through TGA measurements; however, a small amount of graphitic carbon was detected using Raman spectroscopy. In the Raman spectra of all the used catalysts, two peaks were observed at 1580 and 1350 cm^{-1} in the 1200–1700 cm^{-1} region. Both peaks were due to the presence of graphitic carbon in these solids [19].

The absence of carbon deposits, or their formation in very low amounts, in Pt and Rh/La$_2$O$_3$ catalysts and the high stability of the latter make them good candidates for use in membrane reactors.

3.2. Membrane characterization

At 823 K and a trans-membrane pressure of 50 KPa, no He flux through the membrane was observed. This implied the absence of defects in the metal film or sealing leaks and assured 100% selectivity to hydrogen. It is known that hydrogen passes through a Pd-based membrane in a series of steps: first, it adsorbs dissociatively on the surface; then, the surface atomic hydrogen dissolves into the bulk metal; and, finally, at the other side of the membrane, it desorbs as surface atomic hydrogen and recombines as molecular H$_2$ [20]. The permeation of pure hydrogen at 823 K [21] is proportional to the difference in the square root of the feed and permeate pressures. This indicates that the diffusion of the hydrogen through the bulk metal is the rate-limiting step [22].

A H$_2$ permeability study of the membrane was conducted in the empty reactor over a range of temperatures (673–823 K). The results are presented in Fig. 3. The apparent activation energy for hydrogen permeation, calculated from this graph, is 10.2 KJ mol^{-1}. This value compares very well with those for Pd and Pd/Ag membranes previously reported which range from 10.7 KJ mol^{-1} [3] to 23 KJ mol^{-1} [23].
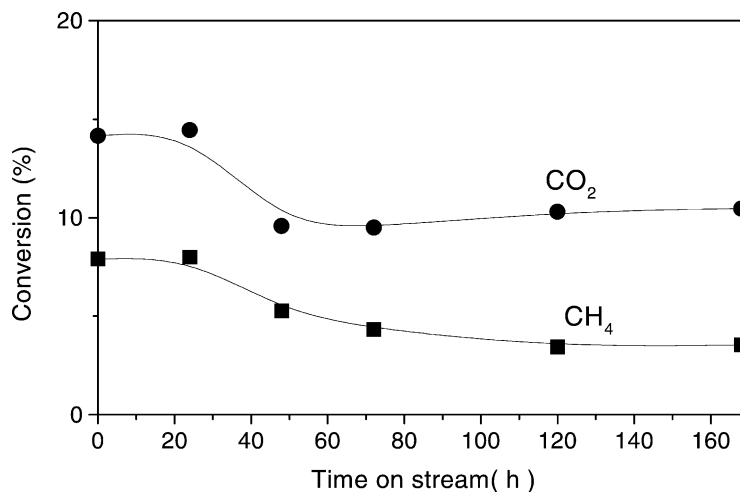
Fig. 2. *Stability test*: Methane (■) and carbon dioxide (●) conversion over Pt (0.93%)/La$_2$O$_3$ supported catalysts. Reaction temperature 823 K, 33 vol.% CH$_4$, 33 vol.% CO$_2$, 34 vol.% He, $P = 1$ atm, $W/F = 1.34 \times 10^{-5}$ g h ml^{-1}.

3.3. Catalysts comparison

3.3.1. Equilibrium conditions

Several research groups have reported the enhancement of the CH$_4$ conversion beyond the limits imposed by thermodynamic equilibrium in the carbon dioxide reforming of methane using membrane reactors [8–12]. The catalytic behavior of Rh (0.2%), Rh (0.6%) and Pt (0.93%) in a membrane reactor is compared in Table 2. Different W/F were employed in order to achieve thermodynamic equilibrium conversion values when the reactor was operated without sweep gas and without pressure drop through the membrane. The observed catalytic activity in a fixed-bed reactor was in the following order: Rh (0.6%) > Rh (0.2%) > Pt(0.93%) (based on TOF values). The results in Table 2 show that when the reactor was operated as fixed bed, it yielded conversions close to thermodynamic equilibrium levels. The use of the membrane configuration resulted
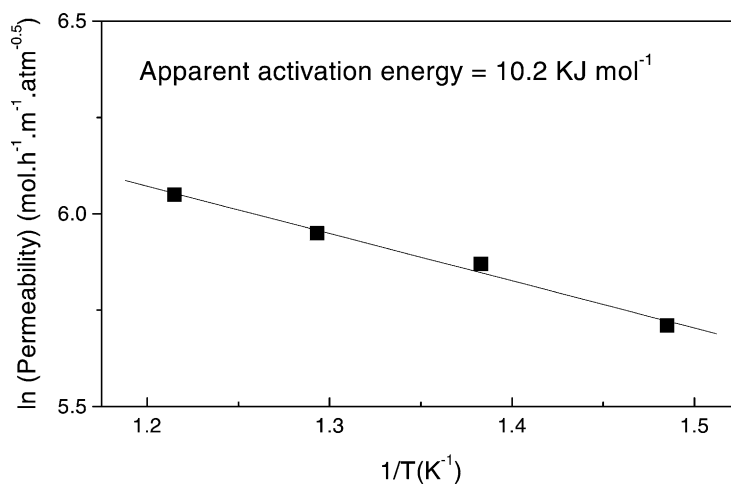

Fig. 3. Temperature dependence of hydrogen flux. $T = 823$ K, pressure drop 20 KPa.

Table 2
Comparison of the La_2O_3 supported catalysts in the membrane reactor

Catalyst	W/F	ΔP (KPa)[a]	Sweep gas (ml min^{-1})	X_{CH_4} (%)[b]	X_{CO_2} (%)[b]	H_2/CO[c]	H_2 permeate (mol h^{-1} m^{-2})
Rh (0.2%)	1.5×10^{-3}	0	0	26.7	37.7	0.47	–
		0	10	31.1	39.8	0.54	6.2
		20	10	29.8	38.0	0.64	9.9
Rh (0.6%)	5×10^{-4}	0	0	26.0	41.9	0.57	–
		0	10	33.9	41.0	0.67	10.1
		20	10	30.7	40.4	0.69	11.5
Pt (0.93%)	3.2×10^{-3}	0	0	26.3	38.2	0.50	–
		0	10	31.3	41.3	0.62	7.9
		20	10	28.9	36.5	0.57	7.9

[a] Pressure difference between the tube and the shell sides.
[b] Feed composition see Table 1. $T = 823$ K, the catalyst was diluted with quartz chips to achieve a bed height of 3 cm.
[c] Total ratio.

in a similar improvement in conversion with all the catalysts.

Kikuchi and Chen [11] found that the activity sequence in a membrane reactor (the permeate was evacuated using a rotary vacuum pump) was different from the one determined in a conventional reactor. They also found an important coke deposition on all the catalysts. Prabhu et al. [8], using stable Ni catalysts, reported similar improvements in methane conversion for Ni/La_2O_3 and Ni/MgO when the plug reactor provided conversions close to equilibrium.

3.3.2. Comparison at equal W/F

Fig. 4 compares the catalytic behaviour of the three catalysts in the membrane reactor at $W/F = 5 \times 10^{-4}$ g h ml^{-1}. Rh (0.6%) has always the highest methane conversion (Fig. 4A) and the highest hydrogen production (Fig. 4B). The highest methane conversion is obtained with no pressure drop through the membrane and 10 ml min^{-1} of sweep gas, an increase of 35% over the equilibrium value being obtained. However, working with the same sweep gas flow and a pressure drop of 20 KPa gives the highest hydrogen flux (Fig. 4B).

3.4. Catalytic behaviour and stability of Rh (0.2%) in the membrane reactor

Since the rates of reaction of CH_4 and CO_2 on Rh (0.2%) and Rh (0.6%) only differ by 10–15% (Table 1) while the amount of Rh changes three times,

the following detailed evaluation of the catalytic performance in the membrane reactor was carried out with the Rh (0.2%) formulation.

3.4.1. Effect of sweep gas

The difference in the hydrogen partial pressure between the reaction and permeation sides is the driving force for H_2 permeation. The rate of hydrogen permeation should be enhanced by the sweeping gas flow rate. The effect of this variable on the level of methane and dioxide conversion for Rh (0.2%) is shown in Fig. 5A. An increase in the flow rate of He reduces the partial pressure of hydrogen at the permeate side, resulting in an increase in the rate of hydrogen permeation through the membrane from the reaction side [24]. The chemical equilibrium of the reforming reaction was considerably shifted to the product side. This is reflected in an improvement of the methane conversion. On the other hand, hydrogen is a reactant for the reverse water–gas shift reaction, so this chemical equilibrium is shifted to the reactant side. Thus, the dioxide conversion remains almost constant with the sweep gas flow rate.

The hydrogen flow through the membrane (permeate side) increases with increasing sweep gas flow (solid line in Fig. 5B). In order to check the membrane permeability, experiments with different H_2/He mixtures were carried out. The effect of the sweep gas on the hydrogen flux through the membrane for 5 and 10% H_2 mixtures is shown in dotted lines in Fig. 5B. The hydrogen mole fraction in the reaction
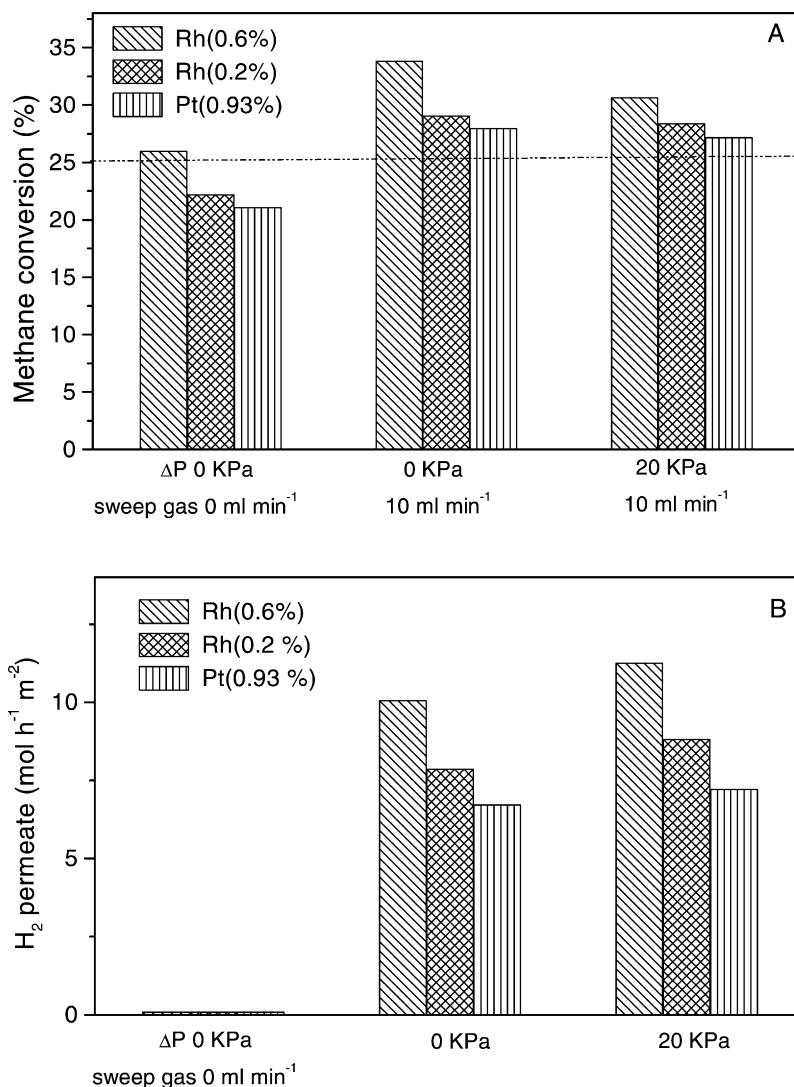
Fig. 4. Catalytic behavior of Rh (0.6%), Rh (0.2%) and Pt (0.93%) in the membrane reactor at 823 K, feed composition (see Fig. 2), $W/F = 5 \times 10^{-4}$ g h ml^{-1}. The dashed line indicates the equilibrium conversion. (A) Methane conversion, (B) hydrogen permeation flux.

side is always between 0.05 and 0.10. The fact that the permeate flux during reaction is between the mixtures fluxes would indicate that the membrane capacity value was reached.

3.4.2. Effect of pressure

In a conventional reactor, an increase of pressure leads to a decreased conversion during the steam reforming but when a dense Pd/Ag membrane is employed, the conversion may increase with pressure due to the selective removal of hydrogen by permeation with increase of pressure [6]. Petersen et al. [7] also found that increasing the reaction pressure was advantageous for steam reforming. A similar effect could be expected for the carbon dioxide reforming in a Pd/Ag membrane reactor. The effect of pressure was studied in a fixed-bed reactor with the Rh (0.6%) solid. A 21% decrease was observed in the methane conversion for a pressure of 80 KPa. Fig. 6 shows that both methane and carbon dioxide conversions
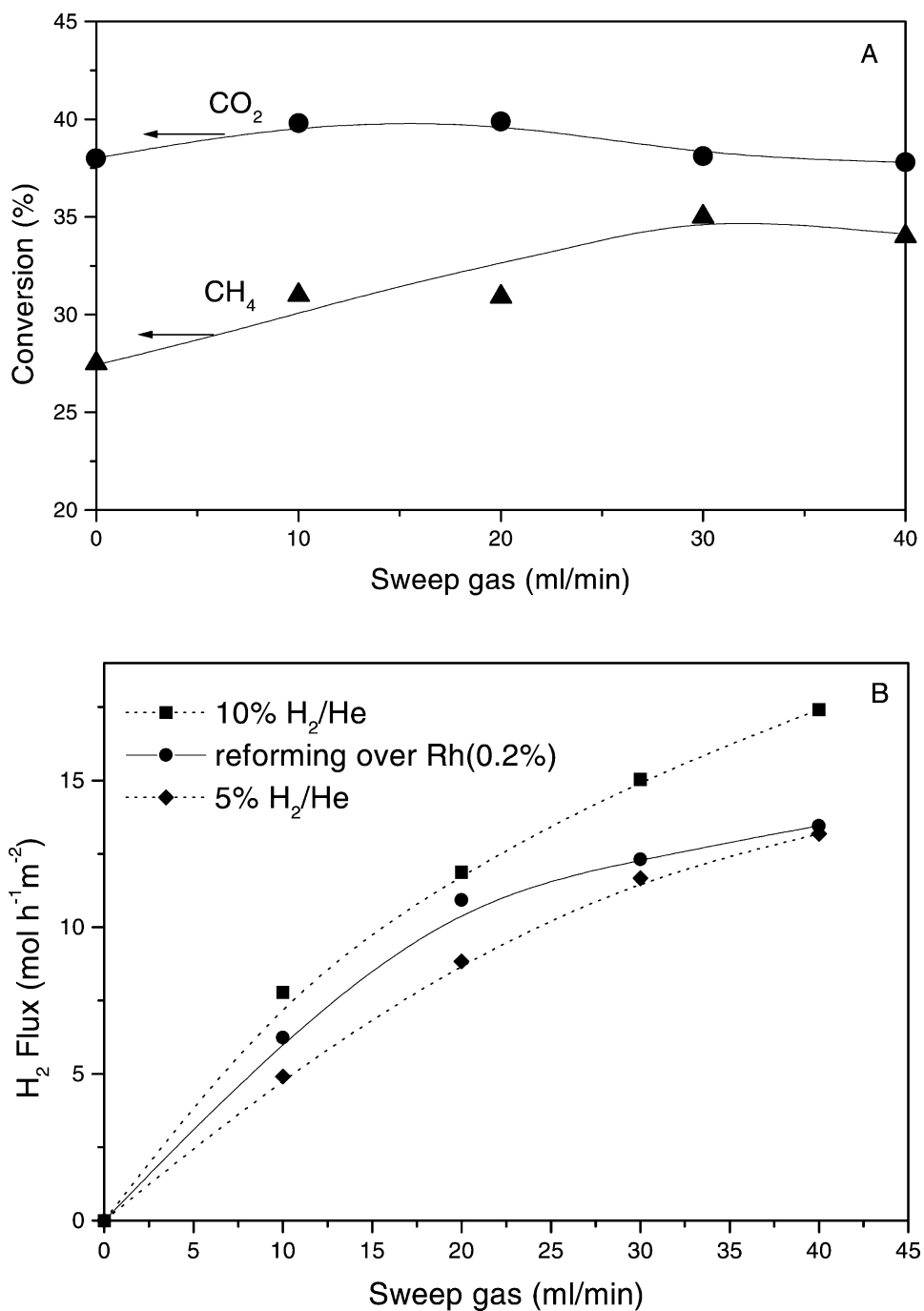
Fig. 5. Effect of the sweep gas flow rate on the behavior of Rh (0.2%), $W/F = 1.5 \times 10^{-3}\,\mathrm{g\,h\,ml^{-1}}$, $T = 823\,\mathrm{K}$, $\Delta P = 0\,\mathrm{KPa}$. (A) Methane and carbon dioxide conversions, (B) hydrogen flux through the membrane.
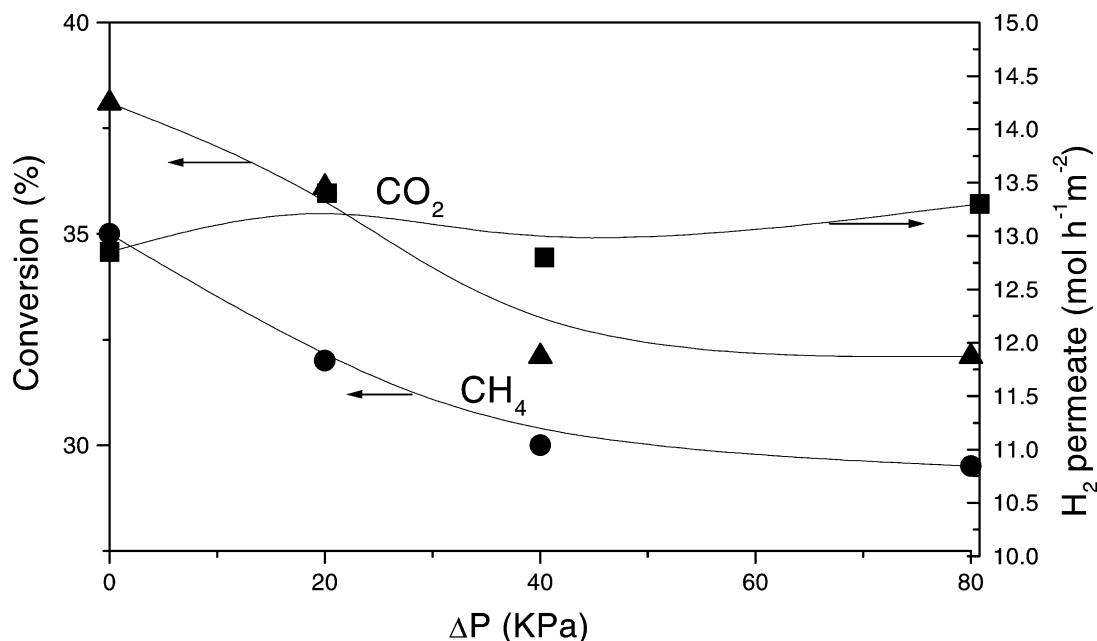
Fig. 6. Effect of pressure on the behavior of Rh (0.2%), feed composition (see Fig. 2), $W/F = 1.5 \times 10^{-3}$ g h ml^{-1}, $T = 823$ K, sweep gas = 30 ml min^{-1}.

decrease with pressure drop through the membrane. The negative effect of the pressure over conversion is dominant and the hydrogen flux remains constant with an increase of pressure drop through the membrane.

3.4.3. Effect of W/F

Table 3 shows the behavior of Rh (0.2%) in the membrane reactor. Three different W/F values were used. At 5.0×10^{-4} g h ml^{-1}, when the reactor was

Table 3
Catalytic behavior of Rh (0.2%) in the membrane reactor

W/F	ΔP (KPa)[a]	Sweep gas (ml min^{-1})	X_{CH_4} (%) (25.2)[b]	X_{CO_2} (%) (43.9)[b]	H_2/CO[c]	H_2 permeate (mol h^{-1} m^{-2})
5.0×10^{-4}	0	0	22.2	29.3	0.55	0.0
	0	10	29.0	38.6	0.64	7.9
	20	10	28.4	35.0	0.66	8.8
1.5×10^{-3}	0	0	26.7	38.0	0.48	0.0
	0	10	31.1	39.8	0.54	6.2
	0	30	35.1	35.1	0.61	12.3
	20	10	29.8	38.0	0.64	9.9
2.5×10^{-3}	0	0	27.0	37.6	0.50	0.0
	0	10	32.8	39.2	0.67	8.8
	0	30	38.0	40.7	0.70	15.8[d]
	20	10	30.2	36.8	0.68	8.8

[a] Pressure difference between the tube and the shell sides.
[b] $T = 823$ K, the catalyst was diluted with quartz chips to achieve a bed height of 3 cm (equilibrium values are given between brackets).
[c] Total ratio.
[d] Calculated ratio: 0.369 mol of permeated H_2 mol^{-1} of feed CH_4.

operated without sweep gas and without pressure drop, methane and dioxide conversion were lower than the theoretical equilibrium values considering the WGS reaction. However, with a sweep gas flow rate of 10 ml min^{-1}, both conversions were increased by 30%. Conversions at $W/F = 1.5 \times 10^{-3}$ g h ml^{-1} (no sweep gas, no ΔP between membrane sides) can be considered equilibrium values because a further increase in W/F did not change those values. These values are in agreement with our results [13] obtained in the fixed-bed reactor. However, they do not coincide with the values calculated when both the $CH_4 + CO_2$ and the reverse WGS reaction were considered. On the other hand, when we used the Rh/ZrO_2 catalysts [25], the measured and calculated values were identical. These observations seem to indicate that another reaction is occurring with the Rh/La_2O_3, which is responsible for the difference between calculated and experimental values.

When starting with equilibrium conversions, the effect of the sweep gas flow was lower; there was an increase of 15–25% in the methane conversion and only 4–5% in dioxide conversion. However, with higher residence time ($>W/F$) and with 30 ml min^{-1} of sweep gas flow rate, the largest equilibrium displacement and the greatest production of H_2 were obtained. Prabhu et al. [10] found an increase of 25% in methane conversion comparing a modified porous glass membrane reactor to a fixed-bed reactor. The conversion in the latter was the theoretical value calculated from thermodynamics.

Galuszka et al. [12] reported the best results; they observed a remarkable increase in the conversion of CH_4 and CO_2 (118 and 92%). These authors found large amounts of filamentous carbon on the spent Pd/Al_2O_3 catalyst. The rate of carbon deposition will remain almost independent of time as long as the metal particle at the tip of the filament is not encapsulated. The formation of filamentous carbon could explain the high conversion values. In the present work, starting from equilibrium conversions of $W/F = 2.5 \times 10^{-3}$ and 30 ml min^{-1} sweep gas flow rate, the CH_4 conversion was increased by 40% (Table 3) and no carbon deposition was observed. The hydrogen permeated per mole of CH_4 was calculated for these conditions. A value of 0.369 mol of permeated H_2 per mol of feed CH_4 was obtained while total H_2 ratio was 0.594.

In addition to the CO_2 reforming, the reverse water–gas shift reaction is taking place and the selectivity towards CO formation is always higher than the selectivity towards H_2. As said before, the reduction in the partial pressure of hydrogen shifts the chemical equilibrium for the reverse water–gas shift reaction to the reactant side. As a consequence, the total H_2/CO ratio is higher in the membrane reactor than in the fixed-bed reactor (Table 3). Galuszka et al. [12] obtained similar results using a composite Pd membrane reactor.

Hydrogen flux through the membrane (Table 3) does not change with the feed flow rate. It is consistent with the fact that the membrane capacity was reached. The highest flux was obtained with high sweep gas flow and without pressure difference across the membrane (Fig. 5B).

3.4.4. Stability

The stability of Rh (0.2%) had already been tested in the fixed-bed reactor [13]. It was also confirmed that in the membrane reactor both the methane conversion and the dioxide conversion did not change after 100 h on stream. ($W/F = 1.5 \times 10^{-3}$ g h ml^{-1}, $T = 823$ K). H_2 permeability measurements were performed to verify that the membrane had not changed during the reaction. Besides, visual inspection of the Pd based membrane did not show any damage or carbon deposition after the reaction tests.

3.5. Characterization of fresh and used catalysts

The TPR data of the Rh (0.2%) and Rh (0.6%) catalysts (Table 1) show two peaks at 481 and 545 K when the solids are pretreated at 823 K in pure oxygen. The Rh/SiO_2 system exhibits a single reduction peak at 395 K [26]. The high temperature TPR peaks in the Rh/La_2O_3 catalysts as compared to the SiO_2 solid indicate that there is a significant interaction between rhodium oxide and the La_2O_3 support. The same effect was reported by Wang and Ruckeinstein [27]. They detected the presence of $LaRhO_3$ in the 10 wt.% Rh/La_2O_3 sample through XRD analysis.

The TPR profiles of all the Pt samples treated at 1123 K present only one reduction peak at temperatures between 590 and 620 K (Table 1). The H_2 consumption indicates that Pt^{4+} is present on these solids. This result is independent of the salt used for impregnation. This means that after high
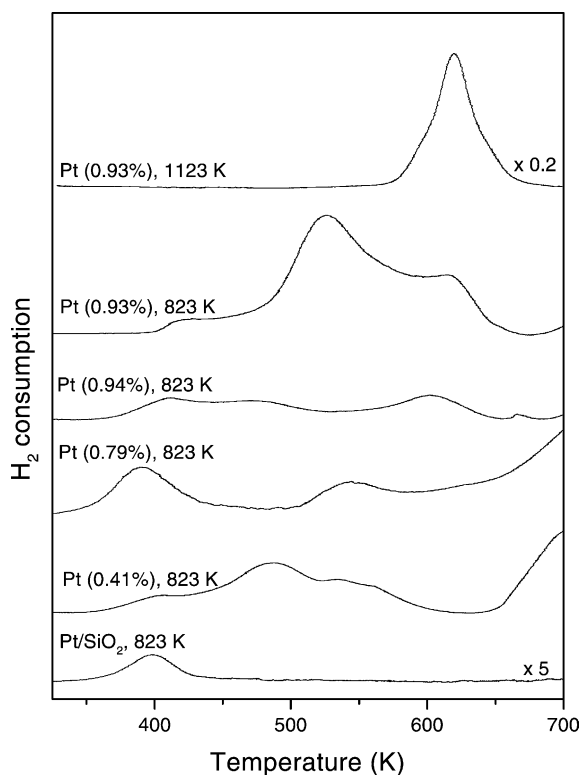
Fig. 7. TPR profiles of calcined Pt catalysts, pretreated in O_2 flow at 1123 and 823 K.

temperature treatment the dominant species is always Pt^{4+}. The Pt/SiO_2 profile presents only one peak at 400 K (Fig. 7), indicating that there is no significant metal-support interaction. No crystalline phases containing Pt are observed on any of the fresh catalysts using XRD. Note that all the catalysts are almost totally reduced at temperatures lower than 700 K.

After treatment at 823 K other features developed in the low loading Pt catalysts. The TPR profiles show several peaks at approximately 420, 480 and 550–610 K (Fig. 7 and Table 1), indicating the presence of different types of metal-surface species. The H_2/Pt ratio was close to 2 for the solids impregnated with chloroplatinic acid. However, when the tretra ammine platinum nitrate was used as impregnation salt, the H_2/Pt ratio was close to one, indicating the almost exclusive presence of Pt^{2+} in this catalyst.

The release of chlorine was investigated through TPD experiments followed with a mass spectrometer. No desorption of chloride species was observed for the calcined samples. Lieske et al. [28] reported that chloride ions remain on the alumina support after reduction to metallic Pt. These ions are available for the formation of $Pt(IV)O_xCl_y$ species from PtO_2 after re-oxidation of the sample.

Bitter et al. [29] reported the TPR of Pt/ZrO_2 after calcination at 925 K. The profile showed two maxima; the first at 472 K is assigned to the reduction of Pt^{4+}. The second at 632 K is attributed to the partial reduction of ZrO_2. When increasing the calcination temperature to 1125 K, no hydrogen uptake was observed during TPR, indicating that Pt was already in the zero-valent state. Thermodynamic calculations indicate that PtO_2 decomposes easily at temperatures above 800 K.

In view of these results, the low temperature peak may be assigned to well-dispersed platinum oxides in the support. The high-temperature peaks could indicate that the reducibility of a platinum fraction decreases by strong interactions with the support or could suggest the formation of halogen-containing surface species.

The literature offers conflicting views about the role of the support and particle size effects for Pt and Rh-based formulations. Bitter et al. [30] reported TOFs of CO_2 at 875 K for Rh catalysts supported on ZrO_2, γ-Al_2O_3 and SiO_2. Through deactivation studies, they concluded that the activity of their catalysts was mainly determined by the availability of Rh and was less influenced by the support. However, Portugal et al. [31] reported that the catalytic behavior of the Rh solids was strongly affected by the nature of the carrier, suggesting that the activity is likely to be related to the different extent of electronic interaction between metal and support. Zhang et al. [32] contend that the initial values of TOF obtained over their supported Rh catalysts exhibit a dependence on particle size, but this dependence might be related to metal-support interactions.

For platinum catalysts, it has been shown [32,33] that the stability of supported Pt catalysts depends strongly on the nature of the support and on its ability to form carbonates.

The CH_4 TOF values previously reported for Pt and Rh catalysts are $<2.0\,s^{-1}$ [32,34,35]. Our activity data show that the catalysts supported on lanthanum oxide present the highest TOFs even at temperatures as low as 823 K.

Catalyst deactivation and the formation of carbon deposits are key factors when the catalysts are to be used in a membrane reactor. The Rh catalyst activity has not been influenced by the carbon deposition after 100 h on stream in a membrane reactor. This behavior could be related to the carbon deposition sites and/or the ability of carbon to play a role as a reaction intermediate [32].

An unusual catalytic stability was reported [36] in Ni supported on lanthanum oxide catalysts. The tight coating of the nickel particles by layers of lanthanum carbonate could hinder the formation of deactivating coke, possibly by limiting the carbon migration through the nickel particles and its recombination as an encapsulating veil around the particle. In our samples, the p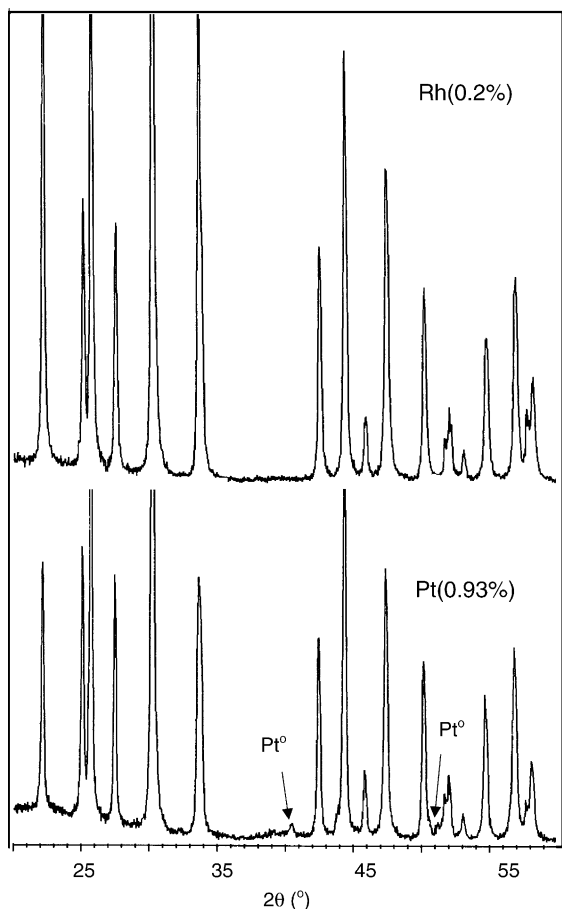resence of surface carbonate species was observed through XPS analysis, in agreement with the bulk XRD results (Fig. 8). The XRD patterns of used samples show the fingerprints of $La_2O_2CO_3$.

In the case of Rh catalysts, the strong interaction between Rh and La oxide is probably responsible for the high stability of these solids. Even though $LaRhO_3$ formation has not been detected in our catalysts, our TPR and XPS data suggest that the stability of Rh (0.2%) is due to the strong metal/support interaction [13].

The deactivation of Pt catalysts has been ascribed to Pt sintering (Pt/SiO_2) [17]and carbon deposition [35]. When lanthanum oxide is used as support, Chen et al. [17] found that a stable amorphous lanthanum oxide could stabilize the Pt to prevent its sintering and could enhance the activation of CO_2 adsorbed on basic sites, facilitating the reforming reaction and hindering the deposition of surface carbon. The presence of Pt^0 reflections (40.7 and 46.3°) in the XRD pattern of used solids (Fig. 8) indicates that platinum was sintered after more than 100 h on stream in the membrane reactor. This is probably the main cause of Pt/La_2O_3 deactivation.

4. Conclusions

(i) Both Pt and Rh catalysts show very low amounts of carbon deposition after more than 100 h on stream.

(ii) The activity of the Rh/La_2O_3 catalysts remains constant after 100 h on stream at 823 K. However, the activity of the Pt/La_2O_3 formulation falls by 1/3 after 50 h on stream.

(iii) The lack of strong metal-support interaction (Fig. 7) favors the sintering of platinum (Fig. 8). On the other hand, the chemical affinity of Rh and La_2O_3 to form rhodates is the basis of the enhanced stability of the rhodium formulations.

(iv) Rh and Pt catalysts significantly increase the conversions of both CH_4 and CO_2 in the membrane reactor. Rh/La_2O_3 is in the long run the most stable and promising formulation. The absence of carbon deposition avoids the deterioration of the membrane observed by other authors [12].

(v) With the membrane reactor, the best results are obtained operating with high W/F values and a sweep gas flow rate of 30 mil min^{-1}.

Fig. 8. DRX pattern of Rh and Pt catalysts after 100 h on stream in a membrane reactor.

Acknowledgements

References

[1] J. Falconer, R. Noble, D. Sperry, in: R. Noble, S.A. Stern (Eds.), Membrane Separation Technology. Principles and Applications, Elsevier, Amsterdam, 1995.

[2] C. Reo, L. Bernstein, C. Lund, Chem. Eng. Sci. 52 (18) (1997) 3075.

[3] S. Uemiya, N. Sato, H. Ando, Y. Kude, T. Matsuda, K. Kikuchi, J. Membr. Sci. 56 (1991) 303.

[4] E. Kikuchi, Y. Nemoto, M. Kajiwara, S. Uemiya, T. Kojima, Catal. Today 56 (2000) 75.

[5] S. Nam, S. Yoon, H. Ha, S. Hong, A. Maganyuk, Korean J. Chem. Eng. 17 (3) (2000) 288.

[6] J. Oklay, K. Hon, R. Hughes, Appl. Catal. A: Gen. 170 (1998) 13.

[7] K. Petersen, C. Nielsen, S. Jørgensen, Catal. Today 46 (1998) 193.

[8] A. Prabhu, R. Radhakrishnam, T. Oyama, Appl. Catal. A: Gen. 183 (1999) 241.

[9] B. Liu, C. Au, Catal. Lett. 77 (2001) 1.

[10] A. Prabhu, A. Liu, L. Lovell, T. Oyama, J. Membr. Sci. 177 (2000) 83.

[11] E. Kikuchi, Y. Chen, Stud. Surf. Sci. Catal. 107 (1997) 547.

[12] J. Galuszka, R. Pandey, S. Ahmed, Catal. Today 46 (1998) 83.

[13] S. Irusta, L. Cornaglia, E. Lombardo, J. Catal. 210 (2002) 7.

[14] J. Bitter, K. Seshan, J. Lercher, J. Catal. 183 (1999) 336.

[15] Y. Chen, B. Liaw, C. Kao, J. Kuo, Appl. Catal. A: Gen. 217 (2001) 23.

[16] K. Nagaoka, K. Seshan, K. Aika, J. Lercher, J. Catal. 197 (2001) 34.

[17] Y. Chen, B. Liaw, W. Lai, Appl. Catal A: Gen. 230 (2002) 73.

[18] M. Mork, W. Maier, J. Catal. 164 (1996) 122.

[19] F. Tuinstra, J. Koenig, J. Chem. Phys. 53 (1970) 1126.

[20] I. Shu, B. Grandjean, A. VanNeste, S. Kaliaguine, J. Chem. Eng. 69 (1991) 1036.

[21] R. Buxbaum, Sep. Sci. Tech. 34 (1999) 2113.

[22] K. Bryden, J. Ying, J. Membr. Sci. 203 (2002) 29.

[23] V. Jayaraman, Y. Lin, J. Membr. Sci. 99 (1995a) 251.

[24] S. Uemiya, N. Sato, H. Ando, T. Matsuda, E. Kikuchi, Appl. Catal. 67 (1991) 223.

[25] S. Irusta, L. Cornaglia, E. Lombardo, J. Catal. 210 (2002) 263.

[26] J. Munera, S. Irusta, L. Cornaglia, E. Lombardo, Latin American Applied Research, submitted for publication.

[27] H. Wang, E. Ruckeinstein, Appl. Catal. A: Gen. 204 (2000) 143.

[28] H. Lieske, G. Lietz, H. Spindler, J. Volter, J. Catal. 81 (1983) 8.

[29] J.H. Bitter, K. Seshan, J.A. Lercher, Top. Catal. 10 (2000) 295.

[30] J.H. Bitter, K. Seshan, J.A. Lercher, J. Catal. 176 (1998) 93.

[31] U. Portugal, A. Santos, S. Damyanova, C. Marques, J.M. Bueno, J. Mol. Catal. A: Chem. 184 (2002) 311.

[32] Z. Zhang, V. Tsipouriari, A. Efstathiou, X. Verykios, J. Catal. 158 (1996) 51.

[33] W. Stagg, E. Romeo, C. Padro, A. Resasco, J. Catal. 178 (1998) 137.

[34] M. Souza, D. Aranda, M. Schmal, J. Catal. 204 (2001) 498.

[35] M. Bradford, A. Vannice, J. Catal. 173 (1998) 157.

[36] A. Slagtern, Y. Schuurman, L. Leclercg, X. Verykios, C. Mirodatos, J. Catal. 172 (1997) 118.